Enhanced immune evasion of SARS-CoV-2 variants KP.3.1.1 and XEC through N-terminal domain mutations

KP.3, a subvariant of JN.1, has rapidly emerged as the dominant strain of SARS-CoV-2 in several countries, and has been designated as a Variant Under Monitoring. Previous studies indicate that the unique Q493E substitution in KP.3 Spike glycoprotein enhances its receptor ACE2-binding affinity and immune evasion, enabling it to outcompete KP.2.[1–6] Notably, KP.3.1.1, which only carries one additional S31 deletion compared to KP.3, has surpassed KP.3 to become the new dominant strain globally (figure A; appendix p 4).[7] Meanwhile, XEC, a recombinant variant of KS.1.1 and KP.3.3, shows strong potential to become the next dominant strain, rapidly expanding across Europe and North America. Compared with KP.3, XEC has only two additional spike mutations, F59S and T22N (appendix p 4).Both S31del and T22N introduce potential glycosylation on the N-terminal domain. Consequently,

Lancet Infect Dis 2024
Published **Online**
November 22, 2024
https://doi.org/10.1016/S1473-3099(24)00738-2

See **Online** for appendix

For more on **covSPECTRUM** see https://cov-spectrum.org

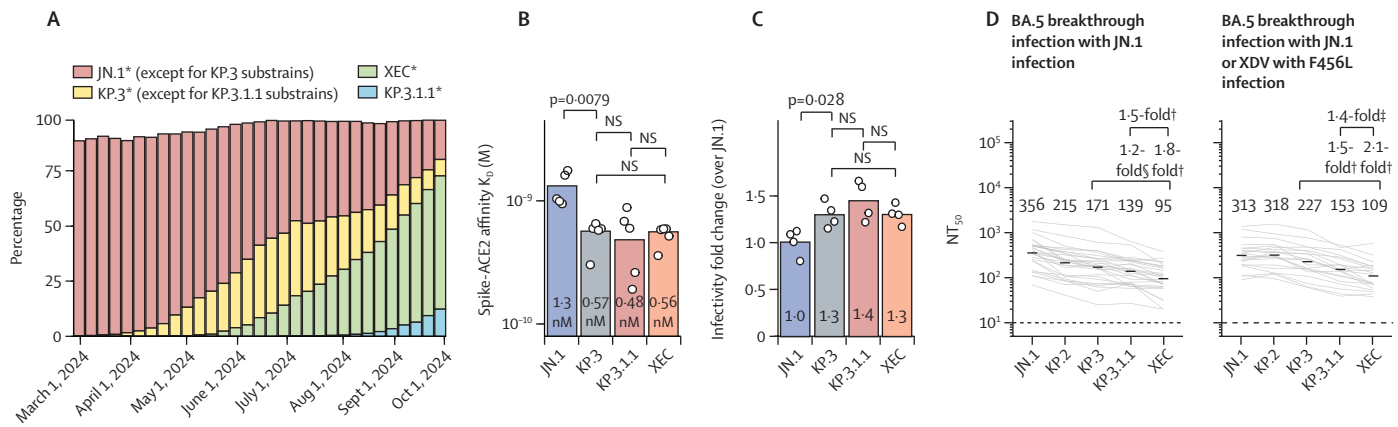

E Pseudovirus IC_{50} (μg/mL)

10^{-3} 10^{-2} 10^{-1} 1

	Soluble ACE2	Class 1									Class 3				Class 1/4				Class 4			Class 5		
		BD57-2669	BD57-3325	BD57-4272	BD57-4298	BD57-4324	BD57-4329	BD57-4347	BD57-4359	BD57-4378	BD57-1895	BD57-4507	BD57-4912	BD57-5304	BD57-4686	BD57-4723	BD57-5252	BD57-5342	BD57-2710	BD57-2847	BD57-3788	BD57-3837	BD57-4734	BD57-4942
KP.3	0·034	0·0012	0·0007	0·0012	0·0036	0·0017	0·0018	0·0009	0·0011	0·004	0·0008	0·0028	0·0015	0·0109	0·0006	0·0009	0·0003	0·0001	0·87	0·86	0·32	0·15	0·21	0·27
KP.3.1.1	0·095	0·002	0·0041	0·0021	0·009	0·005	0·0036	0·003	0·0032	0·0117	0·0014	0·0034	0·0036	0·045	0·0033	0·0028	0·0018	0·0004	0·79	0·67	0·62	0·25	0·26	0·41
XEC	0·075	0·0055	0·0038	0·0089	0·015	0·013	0·0097	0·0032	0·0066	0·0312	0·005	0·0194	0·0094	0·0438	0·0054	0·0057	0·0034	0·0012	0·74	0·76	0·70	0·26	0·35	0·62

IC_{50} fold-change to KP.3

1 3 10

	Soluble ACE2	Class 1									Class 3				Class 1/4				Class 4			Class 5		
		BD57-2669	BD57-3325	BD57-4272	BD57-4298	BD57-4324	BD57-4329	BD57-4347	BD57-4359	BD57-4378	BD57-1895	BD57-4507	BD57-4912	BD57-5304	BD57-4686	BD57-4723	BD57-5252	BD57-5342	BD57-2710	BD57-2847	BD57-3788	BD57-3837	BD57-4734	BD57-4942
KP.3.1.1	2·8	1·7	6·2	1·7	2·5	2·9	2·0	3·5	2·9	3·0	1·7	1·2	2·5	4·1	6·1	3·2	5·7	3·0	0·91	0·78	2·0	1·7	1·3	1·5
XEC	2·2	4·6	5·8	7·2	4·1	7·7	5·4	3·8	5·9	7·9	6·1	7·0	6·3	4·0	9·8	6·5	10·9	9·9	0·86	0·88	2·2	1·8	1·7	2·3

Figure: **Infectivity and antibody evasion characterisation of KP.3.1.1 and XEC**

(A) The percentage of variant sequences circulating globally from March, 2024, to October, 2024, including JN.1 (original JN.1 and its subvariants, excluding KP.3), KP.3 (original KP.3 and its subvariants, excluding KP.3.1.1), KP.3.1.1, and XEC are shown. Data were collected from covSPECTRUM. (B) This chart shows the binding affinity of JN.1, KP.3, KP.3.1.1, and XEC spike proteins to human ACE2, established by surface plasmon resonance. Each circle indicates a replicate. K_D values are displayed within each bar. Two-tailed Wilcoxon signed-rank tests were performed to calculate p-values. (C) This chart shows the relative infectivity of KP.3, KP.3.1.1, XEC compared with JN.1. The pseudovirus infectivity was tested using vesicular stomatitis virus pseudoviruses and Vero cells. Each circle indicates a replicate. Mean values are indicated within each bar. Two-tailed Wilcoxon signed-rank tests were used to calculate the p-values. (D) These graphs show the NT_{50} of convalescent plasma from individuals reinfected with JN.1 after BA.5 or BF.7 breakthrough infection (n=29) and those reinfected with JN.1 or XDV with F456L after BA.5 or BF.7 breakthrough infection (n=21). Geometric mean titres are labelled above each group, with fold changes and statistical significance indicated above the geometric mean titre labels. Paired samples were analysed using a two-tailed Wilcoxon signed-rank test. (E) The first table shows IC_{50} values for a panel of monoclonal neutralising antibodies targeting receptor-binding domain epitopes against KP.3, KP.3.1.1, and XEC mutants. The second table shows the IC_{50} fold-change of KP.3.1.1 and XEC relative to KP.3. IC_{50}=50% inhibitory concentration. K_D=dissociation constant. NS=non-significant (p>0·05). NT_{50}=50% neutralising titre. *Indicates all sublineages. †p<0·0001. ‡p<0·001. §p<0·01.

there is an imperative need to characterise the antigenicity and infectivity of KP.3.1.1 and XEC.

Here we first used surface plasmon resonance to assess the binding affinity between human ACE2 and the Spike of JN.1, KP.3, KP.3.1.1, and XEC. We found KP.3, KP.3.1.1, and XEC showed a significant increase in ACE2-Spike binding affinity compared with JN.1; however, we did not observe significant changes in the receptor binding of KP.3.1.1 and XEC relative to KP.3, despite the N-terminal domain glycosylation mutations (figure B). We then evaluated the infectivity of KP.3.1.1 and XEC using vesicular stomatitis virus-based pseudoviruses in Vero cells. We found that although the pseudovirus infectivity of KP.3, KP.3.1.1, and XEC increased compared with JN.1, no significant differences were observed among KP.3, KP.3.1.1, and XEC (figure C), which is consistent with another recent study.[8]

With the vesicular stomatitis virus-based pseudovirus system, in our study we assessed the neutralisation of convalescent plasma against KP.3.1.1 and XEC, involving plasma samples from two cohorts. Participants in both cohorts received two or three doses of inactivated SARS-CoV-2 vaccines and had breakthrough infections with BA.5 or BF.7. One cohort (n=29) was reinfected by JN.1, and the other (n=21) by JN.1 or XDV with F456L (appendix p11). The specific variant causing reinfections was inferred from local prevalence (>90%) at the sampling timepoint (appendix p6). Of note, XDV shares the same Spike sequence as JN.1. We found that KP.3.1.1 and XEC showed significantly enhanced immune evasion capabilities compared with KP.3 (figure D). Compared with KP.3, the 50% neutralisation titre values against KP.3.1.1 decreased by 1·2-fold in the JN.1 group and 1·5-fold in the JN.1 or XDV with F456L group, whereas against XEC values decreased by 1·8-fold in the JN.1 group and 2·1-fold in the JN.1 or XDV with F456L group. Notably, the JN.1 or XDV with F456L group showed significant plasma neutralisation improvement against KP.2 only, with no differences observed against KP.3, KP.3.1.1, and XEC (appendix p7).

Since KP.3.1.1 and XEC do not have additional receptor-binding domain mutations compared with KP.3, and most neutralising antibodies should target the receptor-binding domain instead of the N-terminal domain, we hypothesised the unexpected strong evasion mediated by the N-terminal domain glycosylation mutations could be attributed to potential effects on the neutralising activity of receptor-binding domain-targeting neutralising antibodies through allosteric effects. Indeed, compared with KP.3, KP.3.1.1 and XEC showed enhanced escape capabilities against neutralising antibodies targeting various epitopes on the receptor-binding domain in Vero cells, especially those competing with ACE2 (figure E; appendix p 8). The inhibition efficiency of soluble ACE2 against KP.3.1.1 and XEC also showed a slight reduction. This enhanced antibody escape capability indicates that the glycosylation mutations on the N-terminal domain of KP.3.1.1 and XEC, located away from the epitopes on the receptor-binding domain, potentially reduce receptor-binding domain-targeting neutralising antibody activity via allostery.

In summary, we found that KP.3.1.1 and especially XEC showed enhanced humoral immune evasion and receptor-binding domain-targeting antibody escape capabilities, supporting the foreseeable dominance of the XEC variant of SARS-CoV-2. However, the mechanisms by which T22N and S31del enhance antibody escape from receptor-binding domain-targeting antibodies remain unclear and require further exploration. The potential mechanisms could involve kinetic changes in receptor-binding domain conformational dynamics induced by additional N-terminal domain glycosylation or effect on membrane fusion efficiency. Further studies are necessary to elucidate the mechanism.

JL and YY contributed equally. YC has provisional patent applications for the BD series antibodies (WO2024131775A9 and WO2023151312A1), and is the founder of Singlomics Biopharmaceuticals. All other authors declare no competing interests.

*Jingyi Liu, Yuanling Yu, Fanchong Jian, Sijie Yang, Weiliang Song, Peng Wang, Lingling Yu, Fei Shao, *Yunlong Cao*
yunlongcao@pku.edu.cn

Biomedical Pioneering Innovation Center (JL, FJ, SY, WS, YC), College of Future Technology (JL), College of Chemistry and Molecular Engineering (FJ), and School of Life Sciences (WS, YC), Peking University, Beijing 100871, China; Changping Laboratory, Beijing, China (JL, YY, FJ, SY, WS, PW, LY, FS, YC); Peking-Tsinghua Center for Life Sciences, Tsinghua University, Beijing, China (SY)

1 Cao Y, Jian F, Wang J, et al. Imprinted SARS-CoV-2 humoral immunity induces convergent Omicron RBD evolution. *Nature* 2023; **614:** 521–29.
2 Yang S, Yu Y, Jian F, et al. Antigenicity and infectivity characterisation of SARS-CoV-2 BA.2.86. *Lancet Infect Dis* 2023; **23:** e457–59.
3 Taylor AL, Starr TN. Deep mutational scanning of SARS-CoV-2 Omicron BA.2.86 and epistatic emergence of the KP.3 variant. *Virus Evol* 2024; **10:** veae067.
4 Wang Q, Mellis IA, Ho J, et al. Recurrent SARS-CoV-2 spike mutations confer growth advantages to select JN.1 sublineages. *Emerg Microbes Infect* 2024; **13:** 2402880.
5 Yisimayi A, Song W, Wang J, et al. Repeated omicron exposures override ancestral SARS-CoV-2 immune imprinting. *Nature* 2024; **625:** 148–56.
6 Yang S, Yu Y, Xu Y, et al. Fast evolution of SARS-CoV-2 BA.2.86 to JN.1 under heavy immune pressure. *Lancet Infect Dis* 2024; **24:** e70–72.
7 Kaku Y, Uriu K, Okumura K, Genotype to Phenotype Japan (G2P-Japan) Consortium, Ito J, Sato K. Virological characteristics of the SARS-CoV-2 KP.3.1.1 variant. *Lancet Infect Dis* 2024; **24:** e609.
8 Prerna A, Happle C, Kempf A, et al. Impact of JN.1 booster vaccination on neutralisation of SARS-CoV-2 variants KP.3.1.1 and XEC. *bioRxiv* 2024; published online Oct 4. https://doi.org/10.1101/2024.10.04.616448 (preprint).